REMOTE SENSING OF VEGETATION FROM UAV PLATFORMS USING LIGHTWEIGHT MULTISPECTRAL AND THERMAL IMAGING SENSORS

J.A.J. Berni [a], P.J. Zarco-Tejada [a], L. Suárez [a], V. González-Dugo [a], E. Fereres [a,b]

[a] Quantalab, Instituto de Agricultura Sostenible (IAS), Consejo Superior de Investigaciones Científicas (CSIC), 14004 Cordoba, Spain - (berni, pzarco, lsuarez, vgonzalez)@ias.csic.es

[b] Dept. of Agronomy, University of Cordoba, Campus Univ. Rabanales, Cordoba, Spain – ag1fecae@uco.e

Introduction

The recent interest of unmanned aerial vehicles (UAV) for vegetation monitoring has been motivated by the benefits of these platforms as compared to full size airborne operation, namely the combination of high spatial resolution and quick turnaround times together with lower operation costs and complexity. These features are of special interest in agriculture where short revisit time is required for management applications and high spatial resolution is mandatory in heterogeneous covers like woody crops. Most of these applications have been possible due to the miniaturization of commercial multispectral and thermal cameras which however require radiometric and geometric calibrations together with atmospheric correction and photogrammetric techniques in order to provide image products similar to the available from traditional airborne sensors. The radiometric quality of the images is critical in order to enable the application of quantitative remote sensing methodologies for a successful estimation of biophysical parameters from remote sensing imagery.

This paper describes the aerial platforms and sensors developed for multispectral and thermal image collection but also focuses on the calibration, postprocessing techniques and further validation of remote sensing products obtained using the combination of the images coupled to radiative transfer models.

System description

Figure 1: Quanta-H, is a rotary wing UAV of 1.9 m main rotor diameter capable of carrying 7kg of payload.

Figure 2: Quanta-G is a fixed wing UAV of 3.2m wingspan with an endurance of 30 minutes flying at 90km/h and available payload of 5.5kg.

Two different types of sensors can be installed on the aerial platforms. The multispectral camera (MCA-6, Tetracam Inc., USA) consists on 6 individual 1.3 Mpixel sensors and optics with interchangeable filters. The filters are selected depending on the vegetation indices (VI) that are required. Figure 3 shows the band centers and width of some of the narrow band filters used in this study.

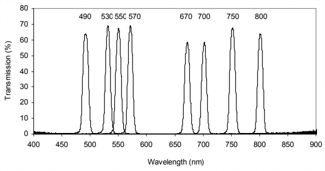

Figure 3: Spectral characteristics of some of the filters used on the multispectral camera.

The thermal camera installed is a Thermovision A40M (FLIR, USA) equipped with a 40º field-of-view lens. The image sensor is a Focal Plane Array (FPA) based on uncooled microbolometers with a resolution of 320x240 pixels and spectral response in the range 7.5-13 µm.

Instrument Calibration

All the cameras have been calibrated in the laboratory following different approaches depending on the type of sensor. In the case of the multispectral camera, a uniform light source consisting on a 50 cm integrating sphere is used to calibrate the camera to radiance. In order to convert the radiance images to reflectance, the SMARTS irradiance model is used to simulate ground surface irradiance. A sun photometer is used to retrieve aerosol optical depth at 6 different wavelengths and total water content. A field validation was conducted measuring with a field spectrometer (figure 4). The results showed an error of 1.17% in absolute reflectance. In the case of the thermal camera, laboratory calibration was conducted using a calibration blackbody source. In order to apply an atmospheric correction, the MODTRAN radiative transfer code is used to model the atmospheric transmissivity and longwave thermal path radiance. Since only vegetation temperature is retrieved, surface emissivity is considered as 0.98 as an accepted value for natural vegetation. The field validation showed absolute errors in the absolute surface temperature of 0.87K after the atmospheric correction was applied (figure 5).

The geometric calibration of the cameras has been performed using Bouguet's camera calibration toolbox. This methodology consists on placing a calibration checkerboard pattern on a fixed location and acquiring several images from different locations and orientations. The grid corner coordinates were extracted semiautomatically from the images, and the intrinsic parameters and exterior orientation (EO) were calculated. In the case of the thermal camera, a calibration pattern was built using resistive wires to obtain a bright pattern when electricity circulated through the wires, thus increasing their temperature. The results of the calibration are the internal parameters of the camera (focal length and principal point coordinates) and a distortion map (figure 6) that can be used to estimate the distortion coefficients for any photogrammetric software.

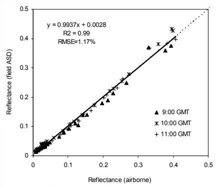

Figure 4. Field validation of the reflectance. The plot shows 90 points from 3 flights over 5 targets for 6 spectral bands.

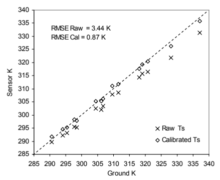

Figure 5. Field validation of the surface temperature. The plot shows the result with and without atmospheric correction.

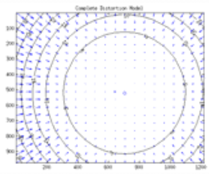

Figure 6. Distortion map generated with the geometric calibration procedure.

Image Products

The INS/GPS data from the autopilot at the exact time of image acquisition is used as an initial approximation for the aerotriangulation (AT). In order to provide a good synchronization of the autopilot data (UTC time) and the image acquisition, a second GPS was used as time source. The image trigger was captured together to the UTC time from the auxiliary GPS receiver using a dedicated microcontroller. The pulse per second (PPS) signal from the GPS was used to ensure time accuracies better than 10ms.

Automatic tie points are extracted using the SIFT algorithm which has shown very robust results as compared with automatic tie point extraction with other photogrammetric software. The images are loaded together with the auxiliary data into the Leica Photogrammetric Suite, where uniformly-distributed ground control points (GCP) were measured throughout the block (figure 7).

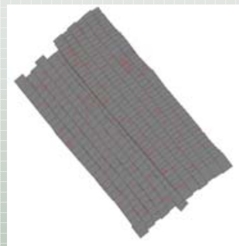

Figure 7: Example of a photogrammetric block of 423 images showing the ground control points with red triangles.

Different image products can be generated from the multispectral imagery calculating different vegetation indexes and using predicting equations obtained from simulations of radiative transfer models that take into account the vegetation properties, canopy architecture or solar and camera geometries (figure 8).

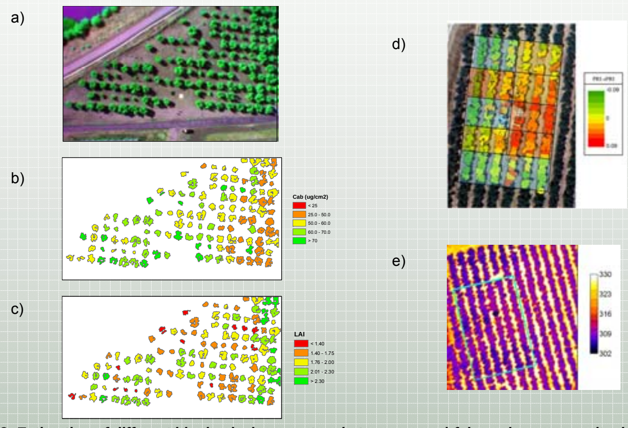

Figure 8: Estimation of different biophysical parameters in tree crops: a) false colour composite; b) chlorophyll content; c) crown LAI; d) pre-visual water stress using PRI; e) canopy temperature.

Conclusions

This work demonstrated that it is possible to generate quantitative remote sensing products by means of a UAV equipped with commercial off-the-shelf (COTS) thermal and multispectral imaging sensors. Laboratory and field calibration methods provided 6-band 10 nm FWHM multispectral imagery with RMSE of 1.17% in ground reflectance and less that 0.2m spatial resolution. For the thermal camera, atmospheric correction methods based on MODTRAN radiative transfer model showed the successful estimation of surface temperature images of 40 cm spatial resolution, yielding RMSE < 1 K.

Photogrammetric techniques were required to register the frame-based imagery to map coordinates. Cameras were geometrically characterized with their intrinsic parameters. These techniques along with position and attitude data gathered from the autopilot enabled the generation of large mosaics semi-automatically with minimum use of ground control points.

Appropriate bandset configurations selected for the multispectral camera enabled the calculation of several traditional narrowband vegetation indices (NDVI, TCARI/OSAVI and PRI), which were linked to biophysical parameters using quantitative methods based on physical approaches such as PROSPECT, SAILH, and FLIGHT models.

The high spatial, spectral and temporal resolution provided at high turnaround times, make this platform particularly suitable for a number of applications, including precision farming or irrigation scheduling, where time-critical management is required.